Measurement of dynamic characteristics of metal sheet under laser shock

Hongbing Yao (姚红兵), Zhusheng Zhou (周祝生)*, Bo Xing (邢 博), Guilin Ding (丁桂林), Yanqun Tong (佟艳群), Jie Ping (平 洁), Liangwan Li (李良湾), and Yongkang Zhang (张永康)

School of Mechanical Engineering, Jiangsu University, Zhenjiang 212013, China

**Corresponding author: senskyzhou124@126.com*

Received September 20, 2011; accepted October 20, 2011; posted online November 18, 2011

A new approach is developed to measure the dynamic characteristics of metal sheet under laser shock, including deformation velocity, strain, and strain rate. The detecting laser beam is partially shaded by the target deformation induced by the laser action. A photodiode transforms the received beam intensity real time into an electrical signal which could record the process of the target deformation. The functional relation between the electrical signal and the deformation of the metal sheet is derived. The deformation curve of a thin aluminum and the velocity curve of its deformation are also obtained during the experiment. The results indicate that the average velocity of the elastic deformation of the target can reach 2.999×10^3 m/s in the central area. This new method provides an approach in the study of the effect of strain rate on deformation.

OCIS codes: 320.7100, 350.4600, 140.3580, 120.1880, 120.7250.
doi: 10.3788/COL201210.043201.

Laser shock forming (LSF) of metal sheets is a new and competitive laser-based manufacturing technology[1]. When a high-power, short-pulse laser acts on a metal surface, plasma with high temperature and pressure is produced in a very short time because of laser energy absorption. Under the restraint layer, the plasma expands and explodes, resulting in a strong shock wave that propagates in the metal. The foregoing is a dynamic response process with high strain rate, so it changes the microstructure and mechanical properties of the metal[2−4]. In the past, the Hopkinson bar and the Taylor impact device have been used to measure dynamic deformation characteristics[5,6]. However, when the target is shocked by laser, the above methods cannot be used effectively because of their narrow response bandwidth. Wang *et al.* conducted experimental measurements and analyses of the dynamic mechanical response of pure aluminum and its spall characteristics using velocity interferometer system for any reflector (VISAR) technology[7]. However, while measuring objects with high acceleration, the received signal frequencies of VISAR exceed the response frequencies of the system. This phenomenon results in signal losses. Moreover, a VISAR system is very expensive, and is difficult to install, commission, and maintain.

In this letter, a photoelectric measurement system using beam shading technique is developed to measure a moving surface with high speed. The detecting laser beam is partially shaded by the target deformation induced by laser action. The deformation curve $d(t)$ of a thin aluminum and the velocity curve of deformation $v(t)$ are obtained in the experiment. Calculations are used to obtain the strain and strain rate of the sheet deformation. Compared with other traditional devices for measuring velocity, this method has better response and is simpler to use.

The experimental setup containing the laser impact and optoelectronic measurement parts is shown in Fig. 1. A Q-switched laser with high power produces a pulse focused on the surface of metal target. A positive-intrinsic-negative photodiode is used to catch a part of the scattered laser as a trigger signal. The probe beam emitted by a semiconductor laser 10 (power: 20 mW; wavelength: 635 nm) is expanded by cylindrical lenses. The expanded beam is shaped by adjustable slit and set parallel to the target plate surface. A narrow-band interference filter (center wavelength: 635 nm) is utilized to scatter light before the probe beam is coupled into photodiode. Convex lens is used to properly focus the light into the photodiode. The light in the photodiode is transformed into an electrical pulse, imported into four-channel digital oscilloscope, and stored in a computer.

In the laser impact aspect of the present study, the laser source is a Q-switched high-power Nd:Glass solid-state laser, with wavelength of 1.06 μm, pulse duration of 10 ns, and spot diameter of 6 mm.

If the plasma blasts freely, the deformation would be tiny and unnoticeable. Thus, a piece of K9 glass is stuck on the metal plate using water as a confinement layer. A confinement layer can increase the impact pressure and extend the duration of an action[8].

When the high-power laser shock acts on the target, the

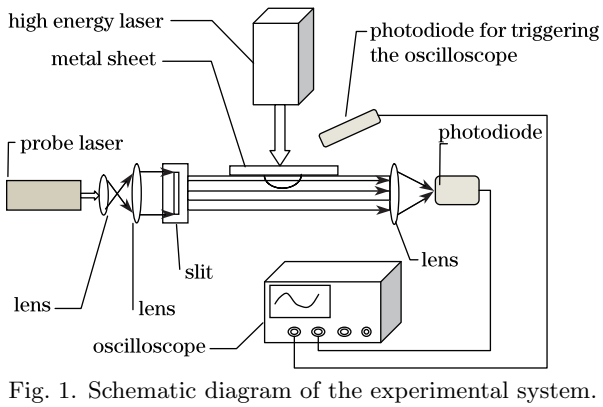

Fig. 1. Schematic diagram of the experimental system.

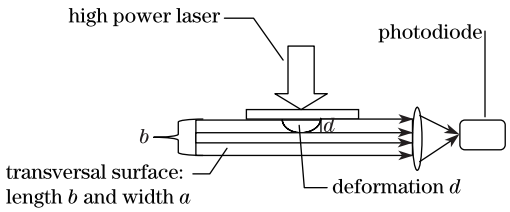

Fig. 2. Deformation of the metal plate under laser shock.

induced deformation of the target changes the received probe laser beam intensity. Therefore, the changes in voltage signal reflect the high-speed forming process of the target.

For our probe laser beam, a Gaussian laser beam generated by a semiconductor laser was used. Its intensity distribution follows a Gaussian function as

$$I = I_0 \exp\left(-\frac{r^2}{r_0^2}\right), \tag{1}$$

where I_0 is the maximum intensity of the probe beam and r_0 is the waist radius. These two are both known parameters.

Let the length and width of the detecting laser cross-section be b and a, and the received flux be Φ. The flux is equal to the integration of light intensity on the uncovered area. After establishing an appropriate coordinate system, we then have

$$\Phi = \iint I \mathrm{d}S = I_0 \int_0^{b-d}\int_{-a}^{a} \exp\left[-\frac{\left(x-\frac{b}{2}\right)^2+y^2}{r_0^2}\right]\mathrm{d}x\mathrm{d}y$$
$$= I_0 \int_0^{b-d} \exp\left[-\frac{(x-b/2)^2}{r_0^2}\right]\mathrm{d}x \int_{-a}^{a} \exp\left(-\frac{y^2}{r_0^2}\right)\mathrm{d}y, \tag{2}$$

where d is the deformation of the metal sheet and $\int_{-a}^{a} \exp\left(-\frac{y^2}{r_0^2}\right)\mathrm{d}y$ is a definite value given as

$$C_1 = \int_{-a}^{a} \exp\left(-\frac{y^2}{r_0^2}\right)\mathrm{d}y. \tag{3}$$

Flux Φ has the following relation with voltage U on the oscilloscope:

$$\Phi = \lambda U + C_2, \tag{4}$$

where λ is the photoelectric conversion coefficient and C_2 is a constant.

Inserting Eqs. (3) and (4) into Eq. (2), Eq. (2) is simplified as

$$\lambda U + C_2 = C_1 \cdot I_0 \cdot \int_0^{b-d} \exp\left[-\frac{(x-b/2)^2}{r_0^2}\right]\mathrm{d}x. \tag{5}$$

Thus, the following equation is obtained as

$$U = \frac{C_1 I_0}{\lambda} \int_0^{b-d} \exp\left[-\frac{(x-b/2)^2}{r_0^2}\right]\mathrm{d}x - \frac{C_2}{\lambda}. \tag{6}$$

Given that $C_1 I_0/\lambda = K$, $C_2\lambda = -C$, Eq. (6) is simplified as

$$U = K \int_0^{b-d} \exp\left[-\frac{(x-b/2)^2}{r_0^2}\right]\mathrm{d}x + C, \tag{7}$$

where parameters K and C are the constants to be determined.

The values of the unknown parameters K and C can be determined in the experiment, shown in Fig. 3.

A screw ruler is placed perpendicular to the probe beam. By spinning the ruler, the laser beam could be shaded with different degrees. The different extents of precession d result in different values of voltage U on the oscilloscope. If the integration part of Eq. (7) is replaced by INT $\left\{\mathrm{INT} = \int_0^{b-d} \exp\left[-\frac{(x-b/2)^2}{r_0^2}\right]\mathrm{d}x\right\}$, then $U = K\cdot\mathrm{INT}+C$ is obtained. Therefore, INT has a linear relation with voltage U. Variables b and r_0 in Eq. (7) are known quantities. For the present experiment, $b =$ 5.4 mm and $r_0 = 5$ mm.

By gradually increasing the extent of precession, the values of d, INT, and U are obtained, as shown in Table 1

By plotting a graph of INT versus U, a straight line could be fitted using the least squares method, whose slope is simply the value of K and whose intercept is the constant C.

The fitted line is represented by Fig. 4. From Fig. 4, $K = 0.06678$ and $C = 0.02595$.

By inserting b, r_0, K, and C in Eq. (7), we have

$$U = 0.06678 \int_0^{5.4-d} \exp\left[-\frac{(x-2.7)^2}{25}\right]\mathrm{d}x + 0.02595. \tag{8}$$

The equation represents the functional relationship between voltage U on the oscilloscope and deformation d of the metal sheet. The graph of the relationship is presented in Fig. 5.

We used a thin aluminum sheet with thickness of 0.25 mm

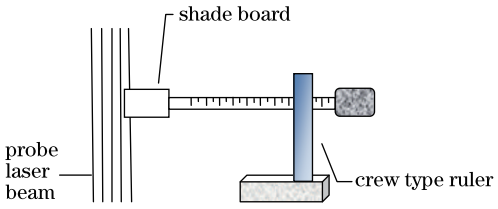

Fig. 3. Experimental determination of the values of K and C.

Table 1. Relationship among d, INT, and U

d (mm)	0	1	2	2.5	3
INT (mm)	4.91802	4.09571	3.15446	2.6589	2.15937
U (V)	0.354365	0.299452	0.236575	0.203479	0.170183
d (mm)	3.5	4	4.5	5	5.4
INT (mm)	1.66579	1.18772	0.733838	0.311437	0
U (V)	0.137278	0.105236	0.074925	0.046772	0.02591

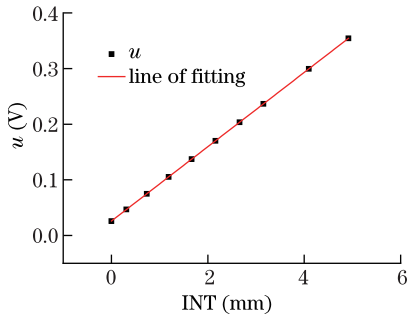

Fig. 4. A straight line fitted using least squares method.

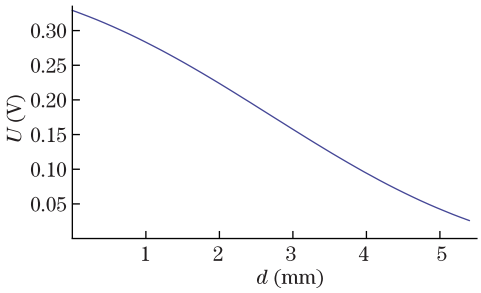

Fig. 5. Relation between voltage U on the oscilloscope and deformation d of the metal sheet.

as the target. The thin aluminum acquires a noticeable plastic deformation when hit by a short-pulse laser with an 8-J energy.

Inserting the data $U(t)$ collected from the oscilloscope into Eq. (8), the aluminum sheet deformation curve $d(t)$ is obtained, as shown in Fig. 6.

Figure 6 presents a saltation at 80 ns (point a), and the signal rises directly to the first wave peak at 2 μs (point b). These findings suggest that when the thin aluminum absorbed the laser energy, successive melting, evaporation, and plasma formation occurred at the laser-focus area. The explosive expansion of the plasma resulted in the emission of shock waves which intensively affected the aluminum sheet and produced a big deformation. The metal sheet underwent a period of plastic deformation after the elastic deformation process. The duration of this process is relatively longer compared with that of the elastic deformation.

For the LSF, the time duration of loading on the metal sheet approaches the order of nanosecond. However, the duration of the deformation intensity in the central area reaching maximum is comparatively longer than the laser-loading process. An analysis of Fig. 6 indicates that the elastic deformation of the aluminum sheet occurred

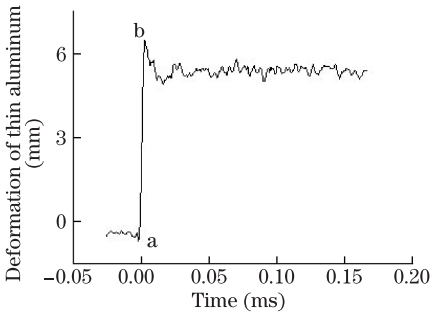

Fig. 6. Aluminum sheet deformation curve.

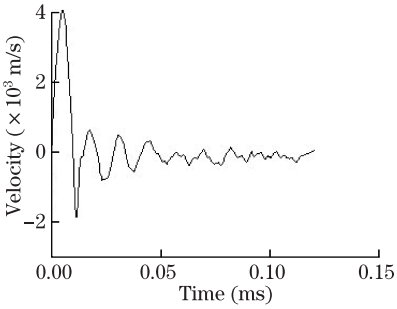

Fig. 7. Velocity curve.

at time point a. The deformation approached its maximum at time point b. The duration is 1.92 μs, and the deformation is 5.7589 mm. Using formula $\overline{v} = \Delta S/\Delta t$, the average velocity of the elastic deformation of the aluminum sheet is 2.999×10^3 m/s in the central area.

The deformation velocity curve of the aluminum sheet is obtained through the differential of the deformation curve. As shown in Fig. 7, at the start of the process, the deformation velocity is fast but it gradually slows down to zero velocity with oscillation.

In conclusion, a novel optoelectronic measurement system is explained. This new method aims to detect the dynamic characteristics of metal sheet under laser shock, including deformation velocity, strain, and strain rate. The experiments conducted yield the deformation history curve of a thin aluminum and the velocity of its deformation. The average velocity of deformation of the target is 2.999×10^3 m/s in the central area. The method involves real-time measurement, so it can be applied to the remote control field under some conditions.

This work was supported by the National Natural Science Foundation of China (Nos. 50735001 and 10804037), the special funded projects of China Postdoctoral Science Foundation (No. 200902506), and the Research Funds of Jiangsu Province Key Laboratory of Photon Manufacture Science and Technology (No. GZ200703).

References

1. L. Zhang, J. Lu, Y. Zhang, K. Luo, F. Dai, C. Cui, X. Qian, and J. Zhong, Chin. Opt. Lett. **9,** 061406 (2011).
2. H. Tan, F. Zhang, J. Chen, X. Lin, and W. Huang, Chin. Opt. Lett. **9,** 051403 (2011).
3. M. A. Meyers, F. Gregori, B. K. Kad, M. S. Schneider, D. H. Kalantar, B. A. Remington, G. Ravichandran, T. Boehly, and J. S. Wark, Acta Materialia **51,** 1211 (2003).
4. C. Yang, Y. Zhang, J. Zhou, L. Zhang, D. Kong, and A. Feng, Journal of Nanjing University of Aeronautics and Astronautics (in Chinese) **37,** (suppl.)1 (2005).
5. Y. Li and K. T. Ramesh, International J. Impact Engineering **34,** 784 (2007).
6. W. Chen, B. Song, D. J. Frew, and M. J. Forrestal, Experimental Mechanics **43,** 20 (2003).
7. Y. Wang, M. Boustie, H. He, T. Sekine, L. Wang, and F. Jing, High Power Laser and Particle Beams (in Chinese) **17,** 966 (2005).
8. Y. Gu, Y. Zhang, X. Zhang, and J. Shi, Acta Phys. Sin (in Chinese) **55,** 5891 (2006).